

Lecture Notes in Electrical Engineering 1257

Zhe Chen
Wenming Yang
Hao Chen *Editors*

2023 International Conference on Energy Engineering

 Springer

Series Editors

Leopoldo Angrisani, *Department of Electrical and Information Technologies Engineering, University of Napoli Federico II, Napoli, Italy*

Marco Arteaga, *Departament de Control y Robótica, Universidad Nacional Autónoma de México, Coyoacán, Mexico*

Samarjit Chakraborty, *Fakultät für Elektrotechnik und Informationstechnik, TU München, München, Germany*

Shanben Chen, *School of Materials Science and Engineering, Shanghai Jiao Tong University, Shanghai, China*

Tan Kay Chen, *Department of Electrical and Computer Engineering, National University of Singapore, Singapore, Hong Kong*

Rüdiger Dillmann, *University of Karlsruhe (TH) IAIM, Karlsruhe, Germany*

Haibin Duan, *Beijing University of Aeronautics and Astronautics, Beijing, China*

Gianluigi Ferrari, *Dipartimento di Ingegneria dell'Informazione, Sede Scientifica Università degli Studi di Parma, Parma, Italy*

Manuel Ferre, *Centre for Automation and Robotics CAR (UPM-CSIC), Universidad Politécnica de Madrid, Madrid, Spain*

Sandra Hirche, *Department of Electrical Engineering and Information Science, Technische Universität München, München, Germany*

Faryar Jabbari, *Department of Mechanical and Aerospace Engineering, University of California, Irvine, USA*

Limin Jia, *State Key Laboratory of Rail Traffic Control and Safety, Beijing Jiaotong University, Beijing, China*

Janusz Kacprzyk, *Intelligent Systems Laboratory, Systems Research Institute, Polish Academy of Sciences, Warsaw, Poland*

Alaa Khamis, *Department of Mechatronics Engineering, German University in Egypt El Tagamoa El Khames, New Cairo City, Egypt*

Torsten Kroeger, *Intrinsic Innovation, Mountain View, USA*

Yong Li, *College of Electrical and Information Engineering, Hunan University, Changsha, China*

Qilian Liang, *Department of Electrical Engineering, University of Texas at Arlington, Arlington, USA*

Ferran Martín, *Departament d'Enginyeria Electrònica, Universitat Autònoma de Barcelona, Bellaterra, Spain*

Tan Cher Ming, *College of Engineering, Nanyang Technological University, Singapore, Singapore*

Wolfgang Minker, *Institute of Information Technology, University of Ulm, Ulm, Germany*

Pradeep Misra, *Department of Electrical Engineering, Wright State University, Dayton, USA*

Subhas Mukhopadhyay, *School of Engineering, Macquarie University, Sydney, New Zealand*

Cun-Zheng Ning, *Department of Electrical Engineering, Arizona State University, Tempe, China*

Toyoaki Nishida, *Department of Intelligence Science and Technology, Kyoto University, Kyoto, Japan*

Luca Oneto, *Department of Informatics, Bioengineering, Robotics and Systems Engineering, University of Genova, Genova, Italy*

Bijaya Ketan Panigrahi, *Department of Electrical Engineering, Indian Institute of Technology Delhi, New Delhi, India*

Federica Pascucci, *Department di Ingegneria, Università degli Studi Roma Tre, Roma, Italy*

Yong Qin, *State Key Laboratory of Rail Traffic Control and Safety, Beijing Jiaotong University, Beijing, China*

Gan Woon Seng, *School of Electrical and Electronic Engineering, Nanyang Technological University, Singapore, Singapore*

Joachim Speidel, *Institute of Telecommunications, University of Stuttgart, Stuttgart, Germany*

Germano Veiga, *FEUP Campus, INESC Porto, Porto, Portugal*

Haitao Wu, *Academy of Opto-electronics, Chinese Academy of Sciences, Haidian District Beijing, China*

Walter Zamboni, *Department of Computer Engineering, Electrical Engineering and Applied Mathematics, DIEM—Università degli studi di Salerno, Fisciano, Italy*

Kay Chen Tan, *Department of Computing, Hong Kong Polytechnic University, Kowloon Tong, Hong Kong*

The book series *Lecture Notes in Electrical Engineering* (LNEE) publishes the latest developments in Electrical Engineering—quickly, informally and in high quality. While original research reported in proceedings and monographs has traditionally formed the core of LNEE, we also encourage authors to submit books devoted to supporting student education and professional training in the various fields and applications areas of electrical engineering. The series cover classical and emerging topics concerning:

- Communication Engineering, Information Theory and Networks
- Electronics Engineering and Microelectronics
- Signal, Image and Speech Processing
- Wireless and Mobile Communication
- Circuits and Systems
- Energy Systems, Power Electronics and Electrical Machines
- Electro-optical Engineering
- Instrumentation Engineering
- Avionics Engineering
- Control Systems
- Internet-of-Things and Cybersecurity
- Biomedical Devices, MEMS and NEMS

For general information about this book series, comments or suggestions, please contact leontina.dicecco@springer.com.

To submit a proposal or request further information, please contact the Publishing Editor in your country:

China

Jasmine Dou, Editor (jasmine.dou@springer.com)

India, Japan, Rest of Asia

Swati Meherishi, Editorial Director (Swati.Meherishi@springer.com)

Southeast Asia, Australia, New Zealand

Ramesh Nath Premnath, Editor (ramesh.premnath@springernature.com)

USA, Canada

Michael Luby, Senior Editor (michael.luby@springer.com)

All other Countries

Leontina Di Cecco, Senior Editor (leontina.dicecco@springer.com)

**** This series is indexed by EI Compendex and Scopus databases. ****

Zhe Chen · Wenming Yang · Hao Chen
Editors

2023 International Conference on Energy Engineering

 Springer

Editors

Zhe Chen 
Aalborg University
Aalborg, Denmark

Wenming Yang
Mechanical Engineering
National University of Singapore
Singapore, Singapore

Hao Chen
Chang'an University
Xi'an, Shaanxi, China

ISSN 1876-1100 ISSN 1876-1119 (electronic)
Lecture Notes in Electrical Engineering
ISBN 978-981-97-7145-5 ISBN 978-981-97-7146-2 (eBook)
<https://doi.org/10.1007/978-981-97-7146-2>

© The Editor(s) (if applicable) and The Author(s), under exclusive license
to Springer Nature Singapore Pte Ltd. 2024

This work is subject to copyright. All rights are solely and exclusively licensed by the Publisher, whether the whole or part of the material is concerned, specifically the rights of translation, reprinting, reuse of illustrations, recitation, broadcasting, reproduction on microfilms or in any other physical way, and transmission or information storage and retrieval, electronic adaptation, computer software, or by similar or dissimilar methodology now known or hereafter developed.

The use of general descriptive names, registered names, trademarks, service marks, etc. in this publication does not imply, even in the absence of a specific statement, that such names are exempt from the relevant protective laws and regulations and therefore free for general use.

The publisher, the authors and the editors are safe to assume that the advice and information in this book are believed to be true and accurate at the date of publication. Neither the publisher nor the authors or the editors give a warranty, expressed or implied, with respect to the material contained herein or for any errors or omissions that may have been made. The publisher remains neutral with regard to jurisdictional claims in published maps and institutional affiliations.

This Springer imprint is published by the registered company Springer Nature Singapore Pte Ltd.
The registered company address is: 152 Beach Road, #21-01/04 Gateway East, Singapore 189721, Singapore

If disposing of this product, please recycle the paper.

Preface

We are delighted to present the proceedings of the International Conference on Energy Engineering (ICEE 2023), held in the vibrant city of Xi'an, China, from December 14–16, 2023. ICEE brought together researchers and professionals from around the world to exchange knowledge, share insights, and discuss the latest advancements in the field of energy engineering.

The 81 papers included in this compilation represent a diverse array of topics, covering key areas such as new transportation energy, power and energy, applied thermal energy, oil and natural gas engineering, and emerging trends in energy research. The contributions within these proceedings reflect the collective efforts of researchers dedicated to addressing the pressing challenges and opportunities in the ever-evolving landscape of energy engineering.

We extend our sincere appreciation to all the authors who submitted their work and the diligent efforts of the peer reviewers who ensured the quality and relevance of the contributions. Special gratitude is also extended to the organizing committee, sponsors, and participants who made this conference a resounding success.

Thank you for all contributions and dedication to advancing the frontiers of energy research.

Contents

Study on Oxidative Exothermic and Pyrolytic Endothermic Characteristics and Kinetics of Chang 7 Medium-Low Maturity Shale Oil Reservoir in the Southern Margin of Ordos Basin	1
<i>Xing Jin, Wanfen Pu, Yuanyuan Bai, and Aoyu Wang</i>	
Correction of Methane Oxidation Kinetic Parameters in On-site Hydrogen Production Based on Combustion Tube Experiments	13
<i>Yuanyuan Bai, Wanfen Pu, Xing Jin, and Huilin Ren</i>	
DG Hosting Capacity Analysis Based on Affine Voltage Sensitivity	22
<i>Yichao Dong, Tianyu Zhang, Tao Luo, Zheng Lei, Dawei Yan, Jia Song, Yuanyuan Li, Dezheng Zhang, Yiwen Chen, and Fengzhang Luo</i>	
Short-Term Industrial Load Forecasting Based on VMD-KELM-Xgboost	31
<i>Jingying Wu, Xiang Zhou, Lili Sun, and Luosong Jin</i>	
A Carbon Reduction Contribution Allocation Method of Distribution Network with Photovoltaic and Storage Devices Based on Carbon Flowing Tracking	42
<i>Yucheng Ma, Qi Wang, Yuxiang Xia, and Bin Chen</i>	
Multi-resource Synergistic Planning Considering Carbon Allowance Trading	55
<i>Jingyu Liu, Zijian Meng, Congyi Wang, Guangzeng Sun, Ming Zhou, and Zhaoyuan Wu</i>	
Analysis of the Influencing Factors of Urban Energy and Electricity Transformation in China Based on Shapley Additive Explanations	64
<i>Zihuan Huang, Weifang Lin, Jun Yi, Maoxin Chen, Zhensong Zeng, and Fengyi Ni</i>	
Compositional Simulation of CO ₂ EOR and Storage in a Low Permeability Oil Reservoir of the Jilin Oilfield	75
<i>Shaoqing Wang, Jinlong Li, Guanyu Zhu, Yu Wang, Ali Maher Noori Satea, and Ye Tian</i>	
Risk Assessment of Change of Important Equipment Management Requirements in Nuclear Power Plant	91
<i>Xipeng Yu and Zhao Wang</i>	

Risk Assessment of Relay Failure in Emergency Diesel Generator of Nuclear Power Plant	101
<i>Xipeng Yu and Liang Pei</i>	
Research on the Recycling Method of Residual Energy from Waste Batteries ...	110
<i>Wei Hu, Mingcai Zheng, Gaoqiang Wu, Liang Zhou, and Zhijun Luo</i>	
Characteristics of Reservoir Rock and Field Tests of EOR Technology in a Tight Oil Reservoir	121
<i>Yaoli Shi, Ling Qu, Ziping Liu, Baocheng Wu, Jianhua Qin, Heng Tian, Di Zhao, Jia Wang, Bin Xie, Liuzhong Li, and Heng Wang</i>	
Composition, Sorption and Stress Sensitivity of Intact and Cleaned Shale Oil Cores	135
<i>Xianghao Meng, Hongye Song, Na Li, Wenguang Feng, and Lei Wang</i>	
Research on Energy Management Strategy Based on Deep Q Learning	150
<i>Ruixin Wang, Dongpeng Guo, and Heng Wang</i>	
Research on Technologies Based on State Grid Management Core	162
<i>Xiaolu Liu</i>	
Validity Standards for Digital Rock Imaging and Analysis	169
<i>Xuejing Guo, Zifei Fan, Heng Song, Jianxin Li, Xuelin Wu, and Fengjun Hao</i>	
Analysis of Energy Storage Value Evolution Considering Cycle Aging Cost ...	184
<i>Zijian Meng, Jingyu Liu, Ming Zhou, Bo Yuan, Lin Chen, and Zhaoyuan Wu</i>	
Bench-Scale Experiments and Field Tests of Water Flooding Among Horizontal Wells with Zipper Fractures in Tight Oil Reservoir	194
<i>Chong Wang, Daixin Chen, Jianming Fan, and Jing Ma</i>	
Research on the Assessment Method of Power Layout in the Context of “Dual Carbon”	207
<i>Zheng Lei, Tianyu Zhang, Yunfei Ma, Dawei Yan, Dezheng Zhang, Tao Luo, Yichao Dong, Jia Song, Yuanyuan Li, Yiwen Chen, and Fengzhang Luo</i>	
A Brief Comparison Between Conventional HVDC and VSC-HVDC Transmission System	217
<i>Jia Song, Tianyu Zhang, Dawei Yan, Jing Xu, Zheng Lei, Yuanyuan Li, and Kui Wang</i>	

A 3Y4 Type Growth Curve Improvement Model and Its Validation	227
<i>Gen Kou, Mingji Shao, HaiYang Liu, Xiang Dai, Bin Yang, Liqiang Wang, Maoxian Wang, Xuejian Xu, and Shuo Yang</i>	
Impact of Oil Degassing on Water-Driven Development Dynamic Indicators ...	238
<i>Zhengshan Qin, Yangyang Ding, Yalan Qing, Wenlong Liu, Yongming He, and Zhihao Chen</i>	
Constitutive Characteristics of Relative Permeability of Tight Sandstone Gas Reservoirs Based on Data-Driven Analyses	253
<i>Yihang Xiao, Zhengtong Du, Lei Wang, Yongming He, Luis R. Rojas-Solórzano, and Zhenjiang You</i>	
Establishing Minimum Economic Field Size for Hydrocarbon Discovery Under Contract Effects	266
<i>Zhi Li, Xu Zhao, Yujin He, Zi Yang, and Fuheng Li</i>	
Modeling the Upgrading Sequence of Conventional Hydrocarbon Reserves	278
<i>Jiawei Wang and Ziyi Zhang</i>	
Dual-Layer Optimization Strategy for Multi-terminal SOPs in ADN Considering Energy Storage Integration	288
<i>Rulei Han, Chao Wang, A. Minfu, and Yuqiang Wang</i>	
Energy Consumption Analysis and Energy-Saving Optimization Operation Research of Air Conditioning Systems in Public Buildings in Jiangsu Province	302
<i>Jinlong Chen, Ying Chen, Min Wu, and Tianqi Wang</i>	
Attenuation and Restoration Characteristics of Ground Temperature in a U-type Deep-Buried Pipe Heat Transfer System	317
<i>Chao Li, Jiale Wu, Jiachen Wang, Hao Chen, Chao Jiang, and Yanling Guan</i>	
Analysis on the Pollution Flashover Cause of Transmission Line Insulators in Inner Mongolia	330
<i>Chuanqiang Che, Baofeng Yan, Jianli Zhao, Jiankun Zhao, Zijian Zhao, and Xiaokai Zhu</i>	
General Modeling of Converter in Power Electronic Distribution System	339
<i>Wei Liu, Ran Cao, Changjun Qu, Xuechang Yu, and Yilin Zhao</i>	

Modeling and Heat Storage Mechanism of Thermal Management Systems
Equipped with Paraffin/expanded Graphite Composite 354
*Abdullah Askari, Raza Gulfam, Saqib Iqbal, Chengbin Zhang,
Mohsin Ali Kazmi, and Izzat Iqbal Cheema*

The Characteristics of Microscopic Heterogeneity and Its Influence
on Imbibition in Shale Oil Reservoirs in Permian Lucaogou Formation,
Jimsar Sag, Junggar Basinjin 364
Yun Wei, Jianbang Wu, Sai Liu, Ziqiang Wang, Yun Luo, and Wenwen Liu

Capacity Optimization and Economic Analysis of an Off-Grid Wind Solar
Hydrogen Production System Including Carbon Trading 378
Xuesong Chang, Bolong Mao, Yingzi Xian, and Lei Wang

Active Damping Optimization Strategy Based on Virtual Pure Resistance 392
Kaixiang Miao, Yuxiao Zhang, Xu Zhao, Yi Wu, and Jianfeng Zhang

Research on the Insulation Characteristics of Nitrogen Insulated Ring
Main Unit 403
*Zhou Baijie, Cai Fanyi, Zhu Zhien, Liu Ji, Tan Dongxian,
and Xiao Dengming*

Experimental Study on Combustion Characteristics of Coal-Based
Naphtha/Ethanol on HCCI Engine 411
Quan Zhang, Ke Yang, and Yujia Kang

Day-Ahead Optimal Scheduling of Combined Wind Power Generation
System Considering the Operation Characteristics of Pumped Storage 419
Yun Tang, Gaojun Meng, Linlin Yu, and Pengfei Yu

Research on Capacity Optimization Configuration of Solar Hydrogen
Production System Based on Layered Optimization Strategy 427
Pengfei Yu, Gaojun Meng, Linlin Yu, and Yun Tang

Optimal Configuration Method of County-Level Integrated Energy
Distribution System for Carbon Power Synergy 435
*Yuchen Zhao, Kai Yuan, Zhenyu Xue, Chongbo Sun, Yifan Sun,
Liwu Gong, Lulu Yang, and Yuguang Zheng*

Research on Data Security Protection of Power Grid Geographic
Information 451
Jing Ma, Jinqiang Fan, Hongyou Chen, and Han Miao

Experimental Investigation on Combustion and Emission of a Common Rail Diesel Engine Fueled with Methyl-Ethyl-Ketone as Port Fuel 458
Jibai Wang, Mingdong Yin, Yangzhi Chen, and Haige Li

Study on Indoor Thermal Comfort of Waiting Hall of Passenger Station in Desert Area in Summer 474
Ying Han, Zhenjie Long, Xiaokai Guo, Kun Li, and Dong Li

Photovoltaic Potential Estimation of Single Building Rooftop Based on High-Definition Map Image and Deep Learning 490
Jie He, Wenbo Cui, Yang Liu, Jinhao Yang, Xiangang Peng, and Baixi Deng

Load and Photovoltaic Power Scenario Extraction Based on Copula Theory and Deep Convolutional Embedded Clustering 504
Yang Liu, Weicong Cai, Jie He, Zhenhuang Wu, Zilu Li, Xiangang Peng, and Baixi Deng

Research on Evaluation Method of Distribution Network Loss Reduction Potential Based on Spatial Distance 520
Jianbin Zhang, Lei Wang, and Zhenhua Xi

Multi-objective Collaborative Optimization Strategy for Distribution Substations with Distributed Photovoltaics 532
Wei Hu, Zhuang Ruan, Xinbo Quan, and Shilei Fang

Experimental Study on Temperature Control and Energy Saving of Reinforced Concrete Silo by Radiative Cooling Technology 545
Linlin Guo, Wenhao Li, Hua Zhang, and Can Yang

Investigation on Ash Melting Characteristics and Additive Co-firing of Coal and Biomass 552
Bin Zhang, Senhao Yang, Guanpeng Li, Xinglin Ji, Tao Luan, and Xun Guo

Seepage Characteristics of Single-Phase Fluids in Tight/Shale Cores 567
Haiyang Liu and Qian Sang

Influence of Energy Consumption Characteristics of Rural Housing on Energy Saving Transformation and Economic Comparison in Severe Cold Area 577
Yuanfang Liu and Junwei Li

Frequency-Voltage Dynamic Modeling and Control of Virtual Synchronous Generators Based Power System	591
<i>Yan Li, Decheng Wang, Qun Zhang, Jian Du, Qinshan Wang, Qiong Wang, Xin Wang, and Zesen Li</i>	
Torque Ripple Suppression for PMSG with Interturn Short Fault Based on Zero Sequence Voltage	598
<i>Yunpeng Cheng</i>	
Research Progress of Three-Dimensional Reconstruction Method Based on Microstructure of Rock	611
<i>Yalong Li, Beining Yang, Zihe Xu, Shicheng Fan, and Yuanlin Zhu</i>	
Assessing Trading Strategies for Distributed Generation Based on Min-Max Regret Approach	626
<i>Jiong Wang, Ye Zhang, Xiangchao Li, Yuan Yuan, Mengyun Wu, Xu Zheng, and Yunting Yao</i>	
Study on the Combustion Characteristics of Diesel/Furan Blended Fuel Based on Visualization	635
<i>Mengyang Ding, Yanfang Liu, and Hao Chen</i>	
Effect of Different Binders on the Mass Transfer Performance of PEMFCs During Cold Start	648
<i>Jie Zhang, Shijing Xie, Dong Huang, and Hao Chen</i>	
An Experimental Study on Velocity Characteristics of the Slug Flow in Gas-Liquid Pipe Flows	659
<i>Siyuan Xu, Hua Li, Jingde Lin, Yinhua Liu, Peihua Zhao, Xingfu Zhong, and Jun Zhang</i>	
Study on Spray Characteristics of Diesel/Furan Blend Fuel Based on Visualization	675
<i>Longkang Che, Yanfang Liu, and Hao Chen</i>	
Preparation of Gas-Suspended Proppant and Field Fracturing Trials	685
<i>Jingchun Zhang, Hongda Ren, Xiangyan Meng, Xiaochuan Tang, and Penghui Jia</i>	
Simulation Research on Thermal Control of Integrated Air Conditioner and Power Battery	694
<i>Yuchen Gu, Keyan Liu, and Xuliang Xie</i>	

Study on Corrosion Resistant Performance of Gas Insulated Switchgear Used in Offshore Wind Power	706
<i>Xiupeng Bao, Liangliang Dang, Yuanxia Li, Weizhi Shao, and Kai Li</i>	
Impact of Port High-Pressure Injection Timing and Direct Injection Timing on Combustion and Emission of Ethylene Glycol/Diesel Dual-Fuel Engine	714
<i>Zhenhua Ji, Fengyu Sun, Yanlei Ma, Ziyi Zhang, Wenbo Zhang, and Hao Chen</i>	
Experimental Study on Combustion and Emission Characteristics of Ethylene Glycol Diesel Dual-Fuel Engine	730
<i>Fengyu Sun, Limin Geng, Hao Chen, Zhenhua Ji, and Wenbo Zhang</i>	
Data-Driven Based Coordinated Voltage Control for Active Distribution Networks with Multiple Devices	745
<i>Shunqi Zeng, Fei Wang, Xin Li, Ziqi Zhang, Yue Zhou, Hao Yu, and Haoran Ji</i>	
Analysis of the Shared Operation Model and Economics of Aggregated Distributed Energy Storage	755
<i>Yu Liu, Na Zhang, Jiali Liu, and Wenting Dong</i>	
Study on Transient Flow Characteristics of an Internal-Mixing Air-Assisted Atomizer Based on Large Eddy Simulation	770
<i>Lin Guan, Yuxuan Wu, Jiling Qiu, Haozhe Shi, Qinglan Zeng, and Genbao Li</i>	
A Planning Method for Distribution System with Integration of Renewable Energy Generation Considering Optimal Distribution Switching	783
<i>Tianyu Zhang, Fengzhang Luo, Zheng Lei, Dawei Yan, Tao Luo, Yuanyuan Li, Jia Song, Denzheng Zhang, Yichao Dong, Yiwen Chen, and Qian Xiao</i>	
Wind Power Correction Prediction Considering Similar Wind Power Climbing Events	794
<i>Kai Li, Kaiming Shi, Ruiming Ma, Shengpeng Sang, Shitong Cao, and Yuliang Gou</i>	
Research on the Planning Methodology of Green Diversified Power Supply Guarantee System Under the Goal of “Dual-Carbon”	807
<i>Yuanyuan Li, Tianyu Zhang, Zheng Lei, Tao Luo, Jia Song, Denzheng Zhang, Yichao Dong, Yiwen Chen, and Fengzhang Luo</i>	

High-Entropy Energy Capture Technology: A Review	816
<i>Ziye Zhang, Hao Chen, Fengyu Sun, Yanlei Ma, Zhenhua Ji, and Wenbo Zhang</i>	
Prediction of Thermal Power Installed Capacity and Power Generation Based on Spearman-PSO and CosHGM(1,1) Model	831
<i>Wenjuan Niu, Jian Tan, Chen Chen, Guiyuan Xue, Xiaojun Zhu, and Zheng Xu</i>	
Modeling and Evaluation of Near Real-Time Carbon Emission Footprint Accounting for Flexible Operation of Coal-Fired Power Units	842
<i>Haoran Li, Bo Li, and Dongjie Xu</i>	
New Method for Calculating Relative Permeability in Low-Permeability and Tight Gas Reservoirs Using Mercury Injection Experimental Data	848
<i>Yangyang Ding, Zhengshan Qin, Yongming He, Wenlong Liu, and Zhihao Chen</i>	
Effect of Gravel Content and Confining Pressure on Mechanical Properties of Conglomerate	863
<i>Ziqiang Wang</i>	
Study on a New Method of Fluid Damage Assessment for Complex Lithologic Reservoir	875
<i>Sai Liu, Gen Kou, Baoxing Liang, Yun Wei, Xiangjun Liu, and Ting Li</i>	
Effects of High-Velocity Flow on the Temperature Field Near the Wellbore: A Review	887
<i>Zhihao Chen, Yangyang Ding, Zhengshan Qin, Yongming He, Baofeng Liang, Yalan Qing, Yisong Xing, and Baihong Li</i>	
Comprehensive Assessment Approach for Reservoir Damage Triggered by Fine Particle Deposition	913
<i>Yisong Xing, Zhengshan Qin, Yangyang Ding, Liu Wenlong, Zhihao Chen, Yongming He, and Baofeng Liang</i>	
Scheduling Model of New Energy Storage System Based on Machine Learning	926
<i>Shiming Li, JiangGang Lv, WenXian Guo, RuiFeng Zhao, Yue Dai, JianDong Tang, Chen Wang, YanLiang Dan, and Wei Zhong</i>	
Study on Constructability Management for Nuclear Power Project	935
<i>Weiting He, Zhenhu Feng, and Rui Ge</i>	

Radioisotope Tracing Technology for Hydraulic Fracturing
of Low-Permeability Shale Oil 945
Yang Pang, Yushou Song, Feng Xu, Guang Wei, Lin Zhao, and Yan Gou

Author Index 955



Study on Oxidative Exothermic and Pyrolytic Endothermic Characteristics and Kinetics of Chang 7 Medium-Low Maturity Shale Oil Reservoir in the Southern Margin of Ordos Basin

Xing Jin¹, Wanfen Pu^{1,2(✉)}, Yuanyuan Bai¹, and Aoyu Wang¹

¹ National Key Laboratory of Oil and Gas Reservoir Geology and Exploitation, Southwest Petroleum University, Chengdu 610500, Sichuan, China
Jinxing19950214@163.com

² Tianfu Yongxing Laboratory, Chengdu 611130, China

Abstract. The amount of recoverable resources by in-situ conversion technology of medium and low maturity shale oil is about $(700\text{--}900) \times 10^8$ t, which is an important replacement resource for oil and gas development. Air injection technology of medium and low maturity shale oil is considered to be an efficient means to improve the recovery of this kind of reservoir. This technology realizes the thermal cracking and transformation of solid kerogen by injecting air and oxidizing organic matter to release a large amount of heat. At present, the oxidation kinetics, thermal endothermic and exothermic characteristics of medium-low maturity shale oil in Chang 7 reservoir in the southern margin of Ordos Basin have not been studied. Chang 7 reservoir was selected as a homogeneous sample, and its pyrolysis and oxidation characteristics in N_2 and Air atmospheres were tested by TG/DTG/DSC, and the relevant activation energy was calculated based on Arrhenius theory. The results show that TOC content of Chang 7 shale oil sample is 21.75%. The oxidative heat release is 8.14 times of the thermal desorption heat, in which the oxidative heat release is 10300.13 J/g, and the thermal desorption heat is 1265.19 J/g. The oxidation and pyrolysis activation energies of the sample are 93.02 kJ/mol and 107.09 kJ/mol, and the pre-factor is $6.73E+09\text{ s}^{-1}$ and $2.71E+14\text{ s}^{-1}$, respectively. The research results provide basic parameters for the numerical simulation of air injection development of Chang 7 reservoir in the southern margin of Ordos Basin.

Keywords: Medium and low maturity shale oil · Oxidation characteristics · Pyrolysis characteristics · Activation energy · Preexponential factor

1 Introduction

China's crude oil consumption and crude oil imports are growing year by year, according to the data of the National Bureau of Statistics of China by 2020, crude oil imports reached 78% of crude oil consumption, and crude oil dependence on foreign countries

is serious [1]. The National Development and Reform Commission and the National Energy Administration jointly issued the “14th Five-Year Plan for Modern Energy System” requiring that oil production should recover to 200 million tons by 2022 and achieve stable production for a longer period of time [2]. In the current “dual carbon” background, China has entered an important period of energy structure transformation. The State Council issued the “complete, accurate and comprehensive implementation of the new development concept to do a good job of carbon peak carbon neutral work” and “2030 carbon peak action Plan Notice”, emphasizing the reasonable regulation of energy consumption, accelerate the development of unconventional oil and gas strategies. Therefore, the accelerated development of unconventional energy is an important guarantee for China’s energy transition.

Shale oil is one of the important unconventional oil and gas resources, which is produced by in-situ conversion of medium and low maturity shale oil and kerogen in oil shale [3]. China’s shale oil resource endowment, low maturity shale oil (maturity between 0.5% and 1.0%) in-situ conversion technology recoverable resources of about $(700\sim 900) \times 10^8$ t [4], is an important oil and gas replacement resources.

However, in medium and low maturity shale oil and oil shale, organic matter mainly exists in the form of solid kerogen, which is difficult to be directly extracted to the surface by existing technology, and needs in-situ modification to transform solid kerogen into free hydrocarbons for exploitation [5–11]. To solve this problem, in recent years, scholars have proposed the air-injected in-situ combustion technology for medium and low maturity shale oil or oil shale reservoir [12, 13]. Its principle is to carry out air-injected in-situ combustion based on a complex pressure fracture network, and convert solid kerogen into free hydrocarbons, such as oil and natural gas, through the heat generated by in-situ combustion, and then exploit the converted free hydrocarbons along the fracture channels. Qin et al. [12] mainly evaluated the air injection development potential of Jimsar shale oil through numerical simulation methods, but they did not test the oxidation/pyrolysis kinetics of kerogen in Jimsar shale oil reservoir. The oxidation kinetic parameters used in the model refer to Lyudmila’s results on Bazhenov Shale Formation [14]. In addition, Chang 7 shale reservoir in the southern margin of Ordos is a medium and low maturity shale oil reservoir, and its pyrolysis hydrocarbon generation kinetics has attracted much attention from scholars [15–19], but there are few reports on its oxidation kinetics, thermal endothermic characteristics and oxidative exothermic characteristics.

Therefore, based on the Chang 7 shale reservoir in the southern margin of Ordos Basin, the heat absorption and heat release characteristics of medium and low maturity shale oil under pyrolysis and oxidation conditions were studied by TG/DTG/DSC technology, and the thermal desorption heat and oxidation heat release heat were calculated. The activation energy and pre-exponential factor of the pyrolysis/oxidation reaction were calculated by Arrhenius theory. The research results provide basic parameters for the numerical simulation of air injection development of Chang 7 reservoir in the southern margin of Ordos Basin.

2 Experimental

First, the sample is treated as powder (> 100 mesh), thoroughly mixed evenly to reduce sample heterogeneity. The total organic carbon content of the sample was measured, and the pyrolysis characteristic curves of the sample under inert atmosphere and the oxidation characteristic curves under air atmosphere were measured by TG/DSC. Based on the integral of DSC characteristic curve, the heat required for pyrolysis and the heat released by oxidation of a unit sample are calculated. It also provides data support for dynamic calculation.

2.1 Samples Preparation

The study sample is black shale, taken from Chang 7 reservoir in the southern margin of Ordos Basin, which belongs to medium and low maturity shale oil, as shown in Fig. 1. The sample was ground to powder by grinding device, and less than 100 mesh powder was screened through a 100-mesh screen, and fully stirred to mix it evenly.

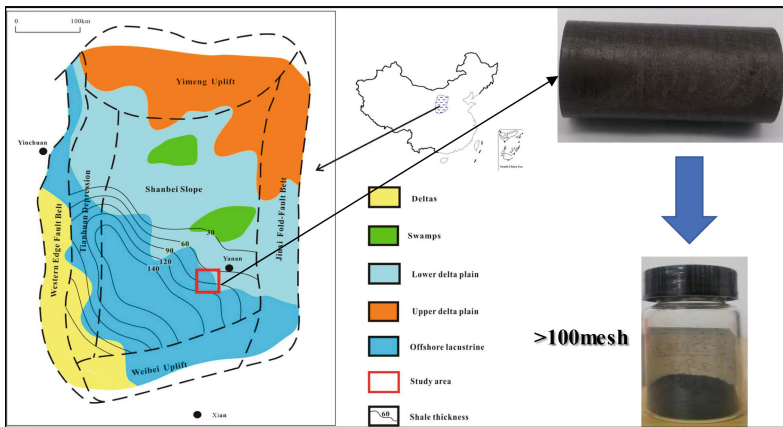


Fig. 1. Sample sampling location and preparation.

2.2 Total Organic Carbon (TOC) Test

Total organic carbon refers to the organic carbon content per unit of sedimentary rock, which is an important parameter to evaluate the amount of oil and gas resources. Free hydrocarbons and solid organic matter (kerogen) usually exist in shale oil reservoirs in medium and low maturity. TOC content is the important factor that determines the heat endothermic of pyrolysis and heat release of oxidation combustion. TOC in the sample was analyzed and studied by the Laboratory Equipment Corporation (type SC832) to determine the pyrolysis/oxidation potential in the sample, as shown in Fig. 2. The TOC analysis method is based on the Chinese national standard the standard that Determination of Total organic carbon in Sedimentary rocks, GB/T 19145-2003.



Fig. 2. Organic sulfur carbon analyzer (Laboratory Equipment Corporation, type SC832).

2.3 Synchronous Thermal Analysis Test

Synchronous thermal analysis combines thermogravimetric analysis (TG/DTG) with differential thermal analysis (DSC). It is a reactor that develops a system to obtain thermogravimetric loss and differential thermal signal of test samples simultaneously under different gas flows. The thermogravimetric and differential thermal characteristics of samples under different gas atmospheres were tested by a synchronous thermal analyzer to clarify the endothermic and exothermic characteristics of the test samples, and to provide experimental data for the calculation of their pyrolysis or oxidation kinetics. The NETZSCH STA 449F3 PC/PG equipped with TG/DSC (Fig. 3 France) was used to conduct synchronous thermal analysis tests on the samples. The test gas types were N_2 and Air, respectively, the heating rate was 10k/min, and the heating interval was 30 °C~600 °C.



Fig. 3. NETZSCH STA 449F3 PC/PG equipped with TG/DSC (France).

3 Kinetic Theory

Organic carbon, a hydrocarbon with very different chemical and physical properties, exists in the form of free hydrocarbons and kerogen. Therefore pyrolysis/oxidation of shale oil with low maturity has a complex phenomenon characterized which many simultaneous reactions. In this study, the kinetic data of pyrolysis reaction/oxidation reaction of shale oil reservoirs with low maturity were obtained by DSC curves in N₂ atmosphere and Air atmosphere. The oxidation or pyrolysis reaction process of low-maturity shale oil is considered to conform to the first-order reaction characteristics, because the gas is always excessive relative to the test sample content (5 to 10 mg) under the development system experiment.

Due to the high sampling frequency of DSC devices in non-isothermal sampling, rapid reactions occurring in infinitesimal time intervals are considered to be isothermal reactions based on differential ideas. Therefore, Formula (1) can be used to characterize the oxidation or pyrolysis reaction rate of low mature shale oil.

$$\frac{d\alpha}{dt} = kf(\alpha) \quad (1)$$

In the above equation, t is the time corresponding to the chemical reaction, s . α is the percentage of the change in energy (mass) in total energy (mass) at a given time. k is the reaction rate constant corresponding to the chemical reaction, s^{-1} . $f(\alpha)$ is a transformation mechanism function. Arrhenius equation is the most important equation of chemical reaction, which is often used to characterize temperature and chemical reaction rate.

$$k = A \exp(-E/RT) \quad (2)$$

In the above equation, A is the Arrhenius constant (referring to the preexponential factor), S^{-1} . T is temperature, k . E is the activation energy of a chemical reaction, kJ/mol . R is the gas constant, $\text{kJ}\cdot\text{mol}^{-1}\cdot\text{K}^{-1}$. The reaction model was considered to be a first-order kinetic reaction, then the corresponding $n = 1$. Therefore, the conversion function can be expressed in the form of Formula (3).

$$f(\alpha) = (1 - \alpha)^n \quad (3)$$

When $n = 1$, it can be seen that the rate of chemical reaction depends only on the reaction rate constant, the energy (mass) of the remaining sample, and the temperature [19, 20]. The essence of the DSC curve is the change of reaction energy corresponding to each moment, so the conversion rate corresponding to the DSC curve at each moment can be calculated by Eq. (4).

$$\alpha = \frac{H_t}{H_0} \quad (4)$$

H_t is the enthalpy released at time t , kJ . H_0 is the total enthalpy released when a chemical reaction terminates, kJ . H is the enthalpy to be released, kJ . The reaction rate equation is expressed in the form of Eq. (5) when Eqs. (2)~(4) are substituted into Eq. (1).

$$\frac{H_t}{H_0} = A \exp(-E/RT) \left(1 - \frac{H_t}{H_0}\right) \quad (5)$$

Equation (5) will be rewritten in the form of Eq. (6) when $H = H_0 - H_t$.

$$\frac{H_t}{H} = A \exp(-E/RT) \quad (6)$$

Take the logarithm of both sides of Eq. (6) to get Eq. (7).

$$\text{Lg}\left(\frac{H_t}{H}\right) = \text{Lg}A - E/2.303RT \quad (7)$$

By linear fitting the relation curve between $\text{Lg}(dH_t/dt/H)$ and $1/T$, the related linear equation can be obtained. The value of E can be obtained from the slope of the linear equation, and the value of A can be estimated from the linear equation intercept. It should be noted that the composition of organic matter in shale oil with medium and low maturity is complicated, which leads to its oxidation and pyrolysis reactions. Therefore, the kinetic data obtained according to Eq. (7) should be considered as apparent parameters.

It must be noted that the chemical stage of medium to low mature shale oil contains multiple reaction regions due to its complex composition. Therefore, if the whole reaction stage is fitted linearly, there may be a phenomenon that the calculation of activation energy is distorted due to poor fitting accuracy. In addition, the individual activation energy of each region does not account for the contribution of each region to the total reactivity. Therefore, the weighted average activation energy E_{wm} is often used to determine the activation energy of the entire reaction stage. The concept of weighted average activation energy E_{wm} was first proposed by Cumming (1982) to determine the overall reaction kinetic parameters of coal samples. Pu et al. (2015) used this method to calculate the total activation energy of crude oil and crude oil + catalyst through TG/DTG/DSC. In this paper, E_{wm} can be expressed as Formula (8).

$$E_{wm} = F_1E_1 + F_2E_2 + F_3E_3 \quad (8)$$

$$A_{wm} = F_1A_1 + F_2A_2 + F_3A_3 \quad (9)$$

where E_{wm} and A_{wm} are weighted average activation energy and Arrhenius constant respectively. E_1, E_2, E_3 and A_1, A_2, A_3 are the single activation energies and Arrhenius constants obtained in each region of the reaction stage, respectively. F_1, F_2 and F_3 are respectively the enthalpy fraction of the combustion material released in each region of the sample.

4 Results and Discussion

4.1 TOC Test Results

The organic sulfur carbon analyzer was used to carry out two tests on the sample, the test sample mass was 0.1030g and 0.0980g, respectively, the test TOC results were 21.9% and 21.6%, and the relative error was 1.4%, as shown in Table 1. The TOC test result was stable, and the average value of the total organic carbon content of the sample was 21.75%.

Table 1. TOC test results.

Number of experiments	Sample weight/g	TOC/%
1	0.1030	21.9
2	0.0980	21.6

4.2 Pyrolysis Characteristics of Medium and Low Maturity Shale Oil

The organic matter in medium and low maturity shale oil reservoir exists as free hydrocarbon and solid kerogen, and free hydrocarbon volatilizes before 300 °C during pyrolysis. After 300 °C, the solid kerogen gradually generates soft asphalt at high temperature, and the soft asphalt is pyrolyzed again at high temperature to form oil and gaseous hydrocarbons. The TG/DTG/DSC characteristic curve tested under nitrogen atmosphere is shown in Fig. 4. The mass loss is 1.8% at 30 °C~300 °C for the thermal volatilization stage, and 15.8% at 300 °C~600 °C for the thermal cracking stage. It shows that most organic matter exists in the form of kerogen, which is consistent with the pyrolysis characteristics of medium and low maturity shale oil.

The non-isothermal absorption curve of DSC is regarded as countless isothermal absorption processes, and the unit isothermal absorption heat is calculated by the formula $W = P \cdot t$, and the heat energy absorbed by the sample in the thermal volatilization and thermal pyrolysis stages is calculated by integrating the time t . Therefore, the relationship curve between DSC and time is drawn by Origin software, as shown in Fig. 5. As can be seen from Fig. 5, all phases from 540 s to 3420 s are endothermic, and its integration is the energy required in the pyrolysis process of medium and low maturity, and the integration result is -1265.19 J/g. Therefore, in the pyrolysis process of this sample, the complete pyrolysis of organic matter in each g sample requires 1265.19 J of heat absorption.

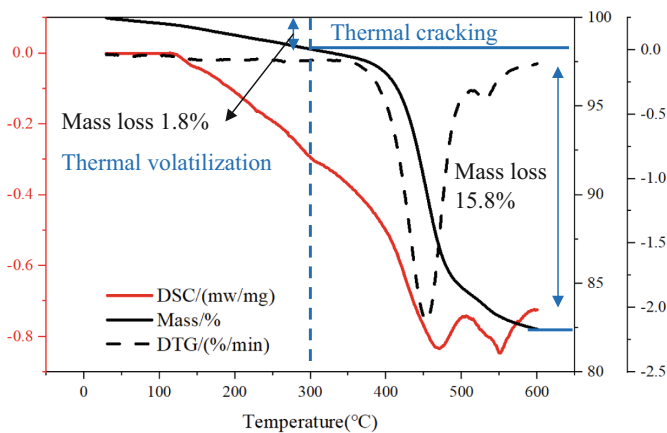


Fig. 4. The relationship between TG/DTG/DSC and temperature in nitrogen atmosphere.

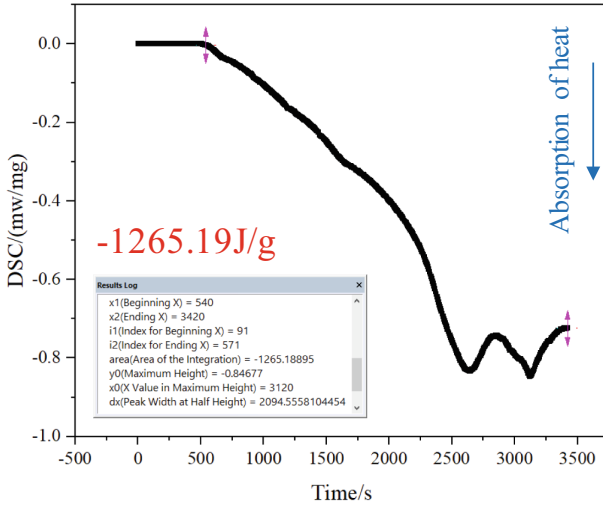


Fig. 5. The relationship between DSC and time in nitrogen atmosphere.

4.3 Analysis of Oxidation Characteristics of Medium and Low Maturity Shale Oil

Due to the complex state of organic matter in medium to low maturity shale oil, the oxidation process becomes intricate. The oxidation of free hydrocarbons, which are low-carbon hydrocarbons, involves a low-temperature oxidation reaction with oxygen, releasing a significant amount of heat. Distinguishing the combustion deposition stage from the oxidation of crude oil is challenging. Therefore, in this study, the oxidation characteristics of medium to low maturity shale oil were divided into two stages: low-temperature oxidation and high-temperature oxidation.

From the relationship curve (Fig. 6) between TG/DTG/DSC and temperature under an air atmosphere, it can be observed that the low-temperature oxidation stage occurs from 30 °C to 383 °C, with a mass loss of 5.1%, which is 3.3% higher than the thermal volatilization stage. The high-temperature oxidation stage occurs from 383 °C to 600 °C, with a mass loss of 24.7%, which is 8.9% higher than the thermal decomposition loss. This indicates that medium to low maturity shale oil experiences greater mass loss during the oxidation process.

The mass loss in the low-temperature oxidation stage can be attributed to the structural transformation of free hydrocarbons. Some adsorbed hydrocarbons or medium to high carbon number hydrocarbons cannot completely volatilize before reaching 300 °C. However, due to the strong reducing properties of oxygen, these hydrocarbons are consumed, leading to a greater mass loss in the low-temperature oxidation stage compared to the thermal volatilization stage. In the high-temperature oxidation stage, apart from the oxidation reaction of kerogen, there is also a reaction with the dead carbon and inorganic carbon in the rock, resulting in a much larger mass loss in the high-temperature oxidation stage than in the thermal decomposition stage.

In addition, both the low-temperature oxidation stage and the high-temperature oxidation stage exhibit exothermic characteristics. By integrating the relationship curve between DSC and time (Fig. 7), the oxidation heat release of medium to low maturity shale oil was determined to be 10300.13 J/g. Therefore, during the oxidation process of the sample, the complete oxidation of organic matter in each gram of the sample releases 10300.13 J of heat. The specific heat release per unit mass in this sample (TOC of 21.75%) is 8.14 times higher than the heat absorption during thermal volatilization.

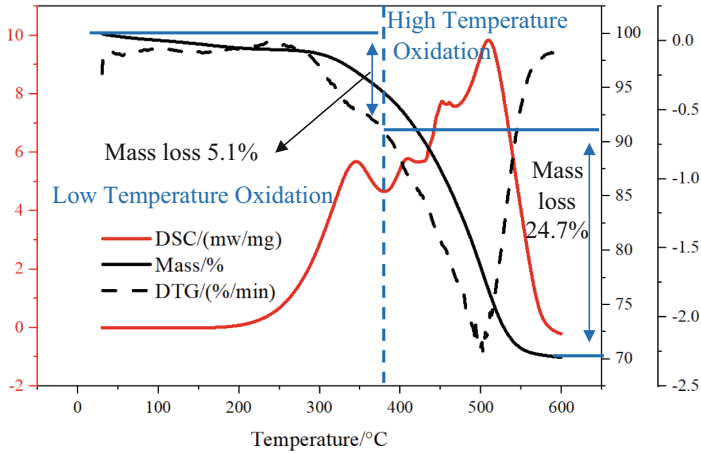


Fig. 6. The relationship between TG/DTG/DSC and temperature in Air atmosphere.

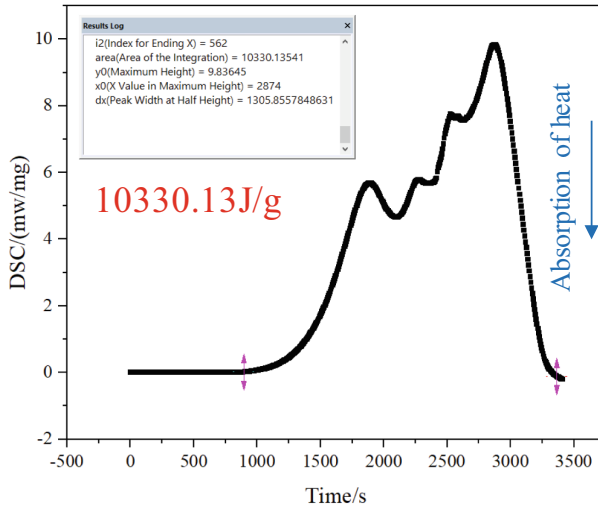


Fig. 7. The relationship between DSC and time in Air atmosphere.

4.4 Kinetic Calculation Result

A relationship curve between $\text{Log}(dH_t/dt/H)$ and $1/T$ was plotted, and the curve was segmented using Origin software (Figs. 8, 9). The segmented fitting of the thermal decomposition kinetics of medium to low maturity shale oil corresponds to fractions F_1 , F_2 , and F_3 , with values of 0.35, 0.34, and 0.31 respectively. Similarly, the segmented fitting of the oxidation kinetics corresponds to fractions F_1 , F_2 , and F_3 , with values of 0.41, 0.31, and 0.28 respectively. The calculated parameters for the thermal decomposition and oxidation kinetics of medium to low maturity shale oil using the kinetic method are shown in Table 2. The activation energy (E) for thermal decomposition is 107.09 kJ/mol, and the pre-exponential factor (A) is $2.71\text{E}+14 \text{ s}^{-1}$. For oxidation, the activation energy (E) is 93.02 kJ/mol, and the preexponential factor (A) is $6.73\text{E}+09 \text{ s}^{-1}$.

From the calculation results, it can be observed that the activation energy for oxidation is lower than that for thermal decomposition in medium to low maturity shale oil. Furthermore, the heat release during oxidation is 8.14 times higher than the heat absorption during thermal decomposition. This indicates that the heat release per unit mass of shale oil oxidized in air is sufficient to meet the energy required for the thermal decomposition of 8.14 units of shale oil per unit mass. These research findings provide a fundamental basis for the in-situ modification of medium to low maturity shale oil by air injection.

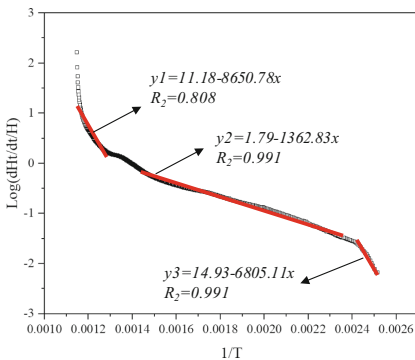


Fig. 8. The pyrolysis kinetics curves were fitted in sections.

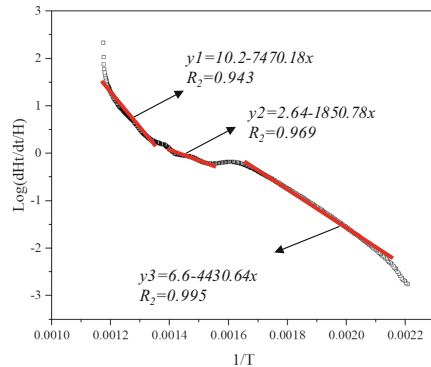


Fig. 9. The curve of oxidation kinetics was fitted in segments.

Table 2. Dynamic settlement results of medium and low maturity shale oil.

Gas type	Activation energy (kJ/mol)				Preexponential factor/ s^{-1}			
	E_1	E_2	E_3	E_{wm}	A_1	A_2	A_3	A_{wm}
N_2	165.64	26.09	130.30	107.09	$1.49\text{E}+11$	62.65	$8.96\text{E}+14$	$2.71\text{E}+14$
Air	143.03	35.44	82.92	93.02	$1.63\text{E}+10$	448.8	$3.96 \text{E}+6$	$6.73\text{E}+09$

5 Conclusion

TG/DTA/DSC technology were used to study the pyrolysis and oxidation characteristics of the medium-low maturity shale oil reservoir Chang 7 in the southern margin of Ordos Basin, and the conclusions are as follows:

The pyrolysis of the sample can be divided into two stages: thermal volatilization and thermal cracking. The temperature of the thermal volatilization stage ranges from 30 °C to 300 °C, and the TG loss is 1.8%. The temperature range of the pyrolysis stage is 300 °C~600 °C, and the thermogravimetric loss is 15.8%.

The sample oxidation can be divided into two stages: low temperature oxidation and high temperature oxidation. In the low temperature oxidation stage, the temperature range is 30 °C~383 °C, and the thermogravimetric loss is 5.1%. The temperature range of high temperature oxidation stage is 383 °C~600 °C, and the thermogravimetric loss is 24.7%.

The oxidation of the sample releases 8.14 times more heat than it absorbs during pyrolysis. The heat released by oxidation was 100300.13 J/g, and the heat absorbed by pyrolysis was 1265.19 J/g.

The oxidation and pyrolysis activation energies of the sample are 93.02 kJ/mol and 107.09 kJ/mol, and the pre-factor is $6.73\text{E}+09\text{ s}^{-1}$ and $2.71\text{E}+14\text{ s}^{-1}$, respectively. It shows that the sample can oxidize at a lower activation energy, which is beneficial to the air injection technology of medium and low maturity shale oil.

Acknowledgement. The authors thank the Tianfu Yongxing Laboratory Science and Technology Research Project (2023KJGG17), Natural Science Foundation of Sichuan Province (2024NSFSC0960). The authors also thank the anonymous reviewers for their constructive and valuable comments.

References

1. Statistics NBO: Statistical Bulletin of the People's Republic of China on National Economic and Social Development for 2022. <http://www.stats.gov.cn/sj/.html>. Accessed 1 Mar 2023
2. Xiaoru, L.: Back to 200 Million Tons, What did Oilmen do Right (1): 200 Million Tons of Return. <http://www.cneo.com.cn/article-42834-1.html>. Accessed 17 Mar 2023
3. Suyun, H.U., Zhao, W., Hou, L., et al.: Development potential and technical strategy of continental shale oil in China. *Pet. Explor. Dev.* **47**(4), 877–887 (2020)
4. Zhao, W., Hu, S., Hou, L., Yang, T., Li, X., Guo, B., Yang, Z.: Types and resource potential of continental shale oil in China and its boundary with tight oil. *Pet. Explor. Dev.* **47**(1), 1–11 (2020)
5. Zhan, H., Yang, Q., Qin, F., et al.: Comprehensive preparation and multiscale characterization of kerogen in oil shale. *Energy* **252**, 124005 (2022)
6. Xu, Y., Lun, Z., Wang, H., et al.: Influences of controlled microwave field irradiation on occurrence space and state of shale oil: implications for shale oil production. *J. Pet. Sci. Eng.* **219**, 111067 (2022)
7. Zhang, C., Cao, J., Xiang, B., et al.: Occurrence state of shale oil in saline lacustrine basins: a lithofacies perspective. *J. Asian Earth Sci.* **255**, 105799 (2023)

8. Liu, X., Yang, W., Li, S., et al.: Occurrence states and quantitative characterization of lacustrine shale oil from Yanchang formation in Ordos Basin. *Res. Inst. Explor. Dev.* **32**(12), 1762–1770 (2021)
9. Zhu, C., Guo, W., Li, Y., et al.: Effect of occurrence states of fluid and pore structures on shale oil movability. *Fuel* **288**, 119847 (2021)
10. Li, S., Li, S., Guo, R., et al.: Occurrence state of soluble organic matter in shale oil reservoirs from the upper Triassic Yanchang formation in the Ordos Basin, China: insights from multipolarity sequential extraction. *Nat. Resour. Res.* **30**(6), 4379–4402 (2021)
11. Andrew, D.H., Moldowan, J.M., Bradley, D.R.: Organic geochemistry of oil and source rock strata of the Ordos Basin north-central China. *AAPG Bull.* **91**(9), 1273–1293 (2007)
12. Jianhua, Q., Tao, W., Jing, Z., et al.: An investigation of in-situ upgrading the shale oil by air injection. In: *SPE Improved Oil Recovery Conference*. Xinjiang Oilfield Company China University of Petroleum-Beijing at Karamay Xinjiang Oilfield Company Texas Tech University (2022)
13. Yang, G., Tao, W., Yan, D., et al.: Numerical and experimental investigation of production performance of in-situ conversion of shale oil by air injection. *Energy Rep.* **8**, 15740–15753 (2022)
14. Khakimova, L., Bondarenko, T., Cheremisin, A., et al.: High pressure air injection kinetic model for Bazhenov Shale formation based on a set of oxidation studies. *J. Pet. Sci. Eng.* **172**, 1120–1132 (2019)
15. Dayong, L., Hengchao, L., Can, Z., et al.: Experimental investigation of pore development of the Chang 7 member shale in the Ordos basin under semi-closed high-pressure pyrolysis. *Mar. Pet. Geol.* **99**, 17 (2018)
16. Han, S., Horsfield, B., Zhang, J., et al.: Hydrocarbon Generation Kinetics of Lacustrine Yanchang Shale in Southeast Ordos Basin, North China. *Energy Fuels* **28**(9), 5632–5639 (2014)
17. Hou, L., Ma, W., Luo, X., et al.: Characteristics and quantitative models for hydrocarbon generation-retention-production of shale under ICP conditions: example from the Chang 7 member in the Ordos Basin. *Fuel* **279**, 118497 (2020)
18. Ma, W., Luo, X., Tao, S., et al.: Modified pyrolysis experiments and indexes to re-evaluate petroleum expulsion efficiency and productive potential of the Chang 7 shale, Ordos Basin, China. *J. Pet. Sci. Eng.* **186**, 106710 (2019)
19. Wang, J.Y., Guo, S.B.: Study on the relationship between hydrocarbon generation and pore evolution in continental shale from the Ordos Basin, China. *Pet. Sci.* **18**(5), 18 (2021)



Correction of Methane Oxidation Kinetic Parameters in On-site Hydrogen Production Based on Combustion Tube Experiments

Yuanyuan Bai^(✉) , Wanfen Pu, Xing Jin, and Huilin Ren

Southwest Petroleum University, Chengdu 610500, Sichuan, China
baiyuanyuan0515@163.com, Jinxing19950214@163.com

Abstract. In numerical simulation studies of methane oxidation, significant errors in simulation results can arise due to the uncertainty of reaction kinetics parameters. Therefore, this study aims to investigate the exothermic behavior of natural gas (primarily methane) oxidation in reservoir environments when injected with hot air (mainly oxygen). The study incorporates experimental data from combustion tube experiments to adjust the kinetic parameters, such as the pre-exponential factor, used in the numerical simulation. By combining experimental and numerical approaches, it is discovered that the significant errors in numerical simulation are primarily caused by the orders of magnitude difference in the pre-exponential factor between the actual experiments and the numerical simulation. Both excessively high and low pre-exponential factors can result in significant errors in chemical reaction rates. After experimental adjustments, the determined pre-exponential factor is $1.09E8$, resulting in a 2.7% error in the methane oxidation kinetic model. Furthermore, the study confirms through dual verification of experimental and numerical simulation that the methane oxidation temperature can reach up to 450 °C. This research not only improves the accuracy of methane oxidation kinetics simulation but also helps deepen the understanding of methane oxidation behavior and mechanisms. It holds significant theoretical and practical implications for optimizing in-situ hydrogen production from natural gas.

Keywords: Methane Oxidation · Kinetic Parameters · Combustion Tubes · Numerical Simulation · Parameter Correction

1 Introduction

The overall strategic goal of China's energy system transformation is to establish a diversified, clean, and low-carbon energy supply system [1]. In this transformation process, hydrogen energy will play an important role, with its characteristics of being a "clean and efficient secondary energy source, flexible and intelligent energy carrier, and green and low-carbon industrial raw material." Currently, over 50% of global hydrogen production comes from natural gas, with even more than 90% in foreign countries [2, 3]. The methods for on-site hydrogen production from natural gas primarily involve the injection of hot air to oxidize hydrocarbons, water-thermal cracking, or reforming into

hydrogen. The exothermic oxidation of natural gas (mainly methane) provides a significant amount of heat for water-thermal cracking in on-site hydrogen production, serving as the foundation and key for efficient hydrogen generation.

Regarding the research on petroleum oxidation and reaction kinetics, many scholars have established kinetic models and conducted extensive studies. Some of these models divide crude oil into pseudo-components for modeling purposes, but in certain situations, the physical properties of these pseudo-components are not explicitly defined [4–12]. Furthermore, some models are only applicable on specific simulators, making it challenging to generalize their use. The calculation of reaction kinetics parameters is usually carried out in a small reaction space, and reservoir numerical simulation is widely used in reservoir scale development. The main challenges in transitioning from experimental reaction dynamics parameters to field scale simulation include the determination of crude oil combustion reaction models and corresponding dynamics parameters, as well as the numerical error of minimizing grid size effects when using large grid blocks in field scale simulation [13, 14]. Zhao Shuai and Barzin et al. [15, 16] also believe that the frequency factors obtained in temperature experiment tests are often inaccurate and need to be substantially adjusted in historical fitting. In recent years, the iso-transformation method has been applied to the analysis of crude oil dynamic parameters [17]. This method can obtain the apparent activation energy without introducing a specific reaction model. After the reaction model is established, typical thermal reservoir simulation can be used to match dynamic parameters and combustion tube experiments [18]. Modeling ISC processes at the field scale presents additional challenges due to the narrow combustion reaction front, which requires centimeter-scale mesh blocks to accurately capture the dynamics. Because the mass and energy conservation equations of commercial heat storage simulators are solved by the Arrhenius kinetic reaction term, the spatiotemporal resolution of the reaction front is poor, so there are serious mesh size effects or numerical errors. Different empirical methods have been used in the past to mitigate this problem, such as adjusting parameters and reservoir temperature values in dynamic calculations [19, 20]. In addition to this, a comprehensive case study of heavy oil in-situ combustion simulation ranging from laboratory experiments to field scale process modeling is conducted. Including dynamic mod-el and combustion tube laboratory experiment, the dynamic reaction model is established, and the experiment is matched historically. Finally, the improved reaction model is used for field simulation. The modified reaction kinetic parameters have been proved to be effective in field scale simulation [21]. This work can provide practical guidance for the predictive numerical simulation and corresponding design of chemical reaction processes. Babushok has tested the kinetic parameters of methane oxidation reaction, and its activation energy is 51.1 kJ/mol and the pre-reference factor is $6.99E6$ [22].

However, further gas reservoir scale simulation needs to be modified by fitting. Based on the above research methods, methane oxidation kinetics was modified through combustion tube experiment and numerical simulation to improve the applicability and accuracy of gas reservoir scale simulation.

2 Experimental Material and Methods

In order to incorporate the methane oxidation kinetics parameters tested in the laboratory into the numerical simulation, the transition from the laboratory parameters to the field scale was carried out. Therefore, combustion tube experiment was used to carry out methane oxidation reaction. The experimental equipment includes combustion tube CT device (Hai'an Petroleum Research Co., LTD) Fig. 1, Gas flowmeter, oxygen cylinder and CH₄ cylinder (concentration 99.99%), CT device contains temperature, pressure control system and electric preheater. The core is prepared into 40–80 mesh cuttings for filling, and the porosity after filling is about 35%. At the beginning of the experiment, the prepared rock cuttings were first filled into the combustion tube, 8 ml water was injected after vacuuming, and then methane gas was injected. The injection was stopped when the injection pressure was 9 MPa, and the confining pressure was always adjusted to be greater than about 2 MPa in the tube, and the ambient temperature was set to 100 °C. After aging for 6 h, oxygen was injected at the rate of 250 ml/min, and the injection amount was 4320 mL (calculated according to the carbon to oxygen ratio 1:1.5). The temperature change of CT tube was recorded at an interval of 1 min.)

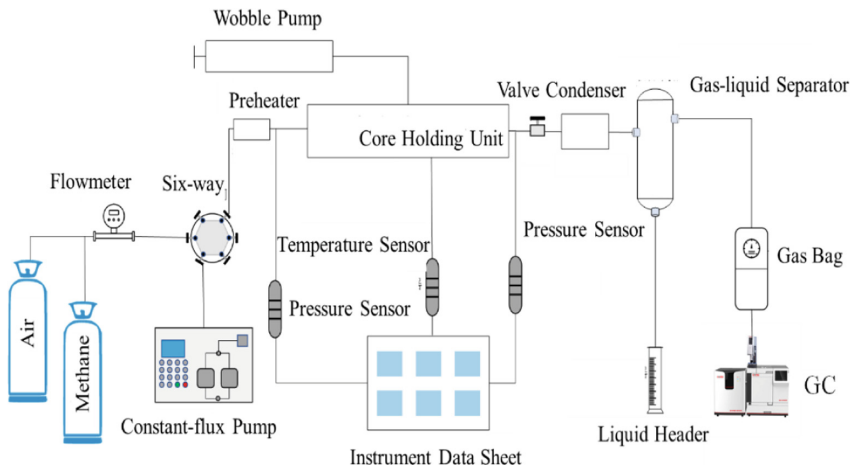


Fig. 1. Schematic diagram of combustion tube device

3 Numerical Simulation and Parameter Correction Methods

CMG-Stars module is used for numerical simulation analysis, and the process of physical experiment can be reproduced by setting simulation conditions. The experimental results, that is, the temperature change caused by methane oxidation reaction, were historically fitted. The core model is divided into radial meshes with a radius of 3.8 cm and a diameter of 10 cm, and the total number of meshes is 1620, as shown in Fig. 2. Thermodynamic parameters of the rock are shown in Table 1 [19]. The fluid model mainly considers